CHAPTER 5
THERMODYNAMIC MODELLING AND COMPARATIVE PERFORMANCE ANALYSIS OF CPC SYSTEM WITH VCRS AND VARS AS BOTTOMING CYCLES

5.1 Introduction

Among all refrigeration systems, the vapor compression refrigeration system (VCRS) is the most commonly used due to its higher COP over the other systems. VCRSs are available in various cooling capacities ranging from few watts to few megawatts. A wide variety of refrigerants can be used in these systems to suit different cooling applications covering a wide range of capacities. Chlorofluorocarbons (CFCs) used in VCRS however cause for concern as they have large ODP and GWP. Use of refrigerants with high ODP and GWP will not be permitted in the near future and low ODP/GWP refrigerants (HFCs and HCs) might be the solutions even though the risk of toxicity or flammability is high with such refrigerants [1].

5.2 Highlight of the works presented in Chapter 3 and Chapter 4

In Chapter 3 and Chapter 4, the energy and exergy analyses performed on the combined RRVPC and single effect $H_2O-LiBr$ VARS was presented and described in detail. In Chapter 3, performance parameters such as net power and efficiency of the toping RRVPC and COP of the bottoming VARS were determined under various operating conditions of FFR, BP, VARS CL and component's operating temperatures. Additionally, a performance comparison between the combined plant and the plant without VARS was provided. The same combined power and cooling system was analyzed from the second law point of view in Chapter 4; where power cycle and VARS exergetic efficiency, exergy efficiency of the combined cycle and irreversibility in various system components were evaluated and presented along with the first law based performance parameters. The energy and exergy based parametric analysis in Chapter 3 and Chapter 4 gave a detailed insight on the influence of the system variables on performance of the CS. It was observed that the net power of the topping power cycle was directly proportional to FFR; however it also led to increase in the irreversible losses in the power cycle components. Further it was found that FFR and BP variation had little impact on efficiency of the power cycle and virtually no impact on VARS performance and its components' irreversibility except in the generator. The generator irreversibility

was less at higher BP and it was the lowest at 150 bar. Irreversibility distribution among various power cycle components showed that the flue gas leaving the boiler, the boiler, cooling tower pumps, steam turbine and cooling tower were the major contributors of irreversibility. Compared to the power cycle components, the irreversibility contribution of the VARS components were less. Exergy destruction in the generator was the highest among the VARS components followed by that of the absorber, condenser and the evaporator.

5.3 Motivation and objective of the work presented in this chapter

Large amount of cooling is required in almost all industrial installations including that of power plants. In most of the power industries/plants, cooling is mainly achieved through use of VCRS driven by high grade electric energy produced indigenously in the power plants. Therefore it may be relevant that a CPC system be analyzed to evaluate its performance with a VCRS integrated to provide the cooling in the plant. In this chapter, we provide thermodynamic analysis (energy and exergy) of a combined RRVPC and a VCRS based cooling system; detail system configuration is discussed later in section 5.4. Since often comparison is provided between VCR and VAR systems [2−4] and although some of the facts are known, still a comparison between VARS and VCRS based combined vapor power and cooling system is possible considering that neither a thermodynamic analysis comparing two combined ST based power and cooling systems is available nor it was attempted before from this point of view. Although the advantages and disadvantages of the VCRS and VARS separately are known, but when they are integrated with the topping power cycle it will depend upon many other factors, most importantly the change in configuration and accordingly the performance of the power cycle will vary. Thus the main objective of the work presented in this chapter is to provide a comparative energy and exergy analysis between the combined power and cooling systems with VCRS and VARS as bottoming cycles. The study quantifies the difference in performance of the topping VPC and the bottoming cooling system for the same operating conditions.

5.4 Description of combined RRVPC and VCRS

The configuration of the CPC system integrated with a VCRS is shown in Fig. 5.1. Fig. 5.2 is the corresponding T−s diagram of the topping RRVPC. The topping RRVPC of this CS is more or less similar with the one that was described in Chapter 3

(Fig. 3.1); however, in this VCRS based configuration, no steam from the ST is extracted. One mixing chamber (MC) and a boiler feed pump (BFP) have been removed from the topping RRVPC of the VARS based CPC system in Fig 3.1 to obtain this new VCRS based CPC system (Fig. 5.1). The piping network, which was required in the VARS based configuration (Fig. 3.1 in Chapter 3) for carrying cold water from cooling tower (CT) exit to the absorber and then hot water from the absorber to the mixing chamber, is not required in the VCRS based CPC system. The electricity produced by the topping RRVPC is the source of energy for the compressor of the VCRS. Moreover, there were total three mixing chambers viz. MC1, MC2 and MC3 in the VARS based system (Fig. 3.1) whereas in the present VCRS based combined configuration (Fig. 5.1), there are only two mixing chambers namely MC1 and MC2, which are identical of MC2 and MC3 in Fig. 3.1. Similarly the total number of BFPs in the VCRS based CPC system (Fig. 5.1) is three compared to four numbers of BFPs in the VARS based configuration in Fig. 3.1. The piping network, which was required in the VARS based configuration (Fig. 3.1 in Chapter 3) for carrying cold water from cooling tower (CT) exit to the absorber and then hot water from the absorber to the mixing chamber, is not required in the VCRS based CPC system.

5.5 Assumptions

The assumptions made and other thermodynamic equations formulated for analysis of the topping RRVPC are almost similar to the ones mentioned in Chapter 3 and Chapter 4; hence, the details about these are not included in this chapter. Fuel thermo−mechanical exergy and air chemical exergy are assumed to be zero. Thermo−mechanical exergy of humid air stream at boiler inlet, at inlet and exit of the CT and AC apparatus is calculated using equation taken from Ref. [5].Since the system schematic in Fig. 5.1 is different from Fig.3.1 due to less number of components and no provision of steam extraction from ST, hence, the state points shown in the VCRS based schematic in Fig. 5.1 are different and accordingly there will be some change in the mathematical equations. The calculation procedure of few important performance parameters of the topping RRVPC and bottoming VCRS is detailed in the following sections. The parameters assumed for system simulation are shown in Table 5.1.

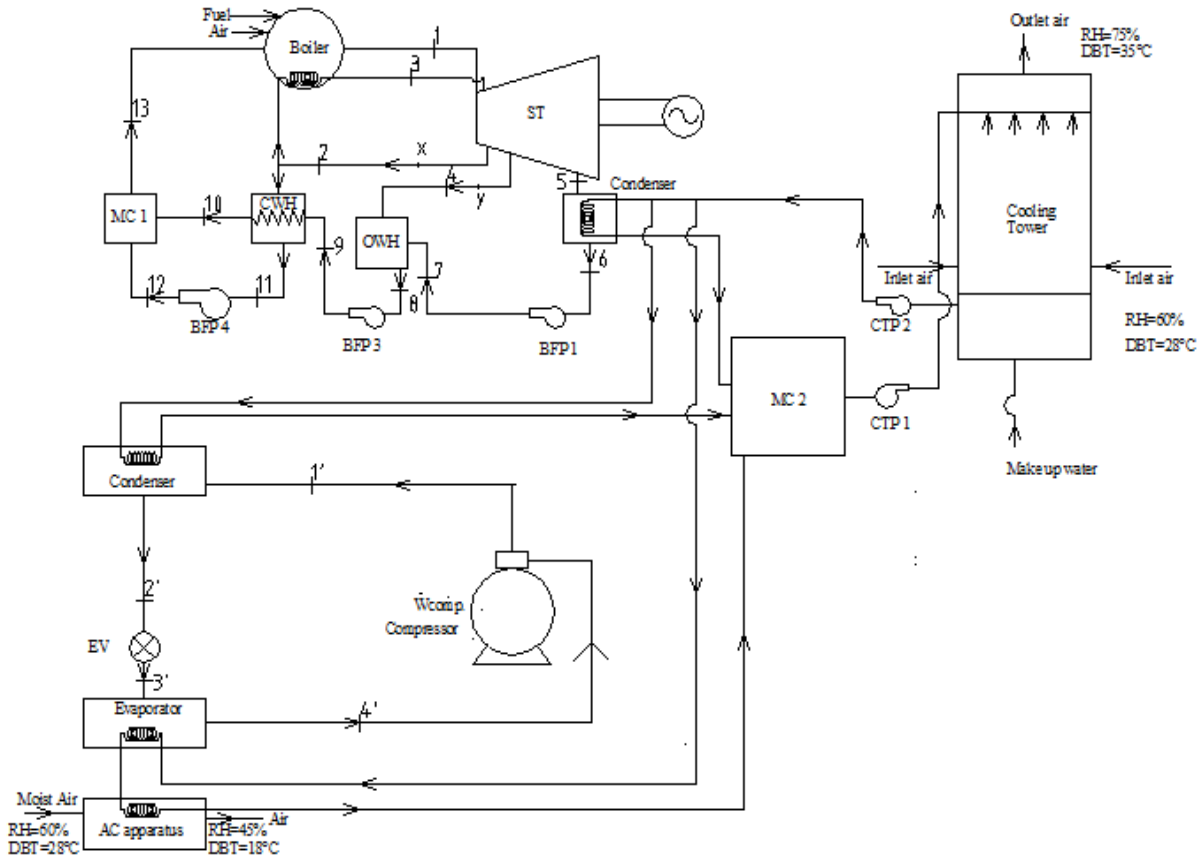

Fig. 5.1: Schematic of the combined RRVPC and VCRS

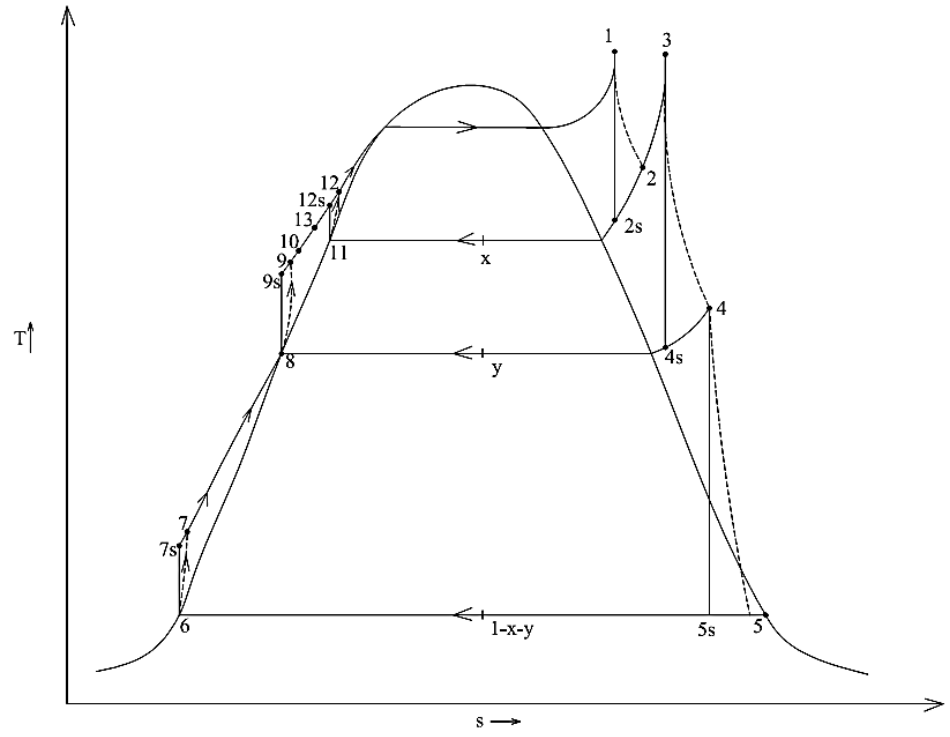

Fig. 5.2: T−s diagram of the power cycle corresponding to Fig.5.1

5.6 Thermodynamic calculations

5.6.1 Calculations: topping RRVPC

The composition of coal used as fuel in the boiler is the same as outlined in Chapter 3 i.e. Carbon (C) 60%, Hydrogen (H) 4%, Oxygen (O) 3%, Nitrogen (N) 2%, Sulphur (S) 3%, Moisture (H_2O) 4% and Ash content 24%.Fuel lower heating value $\left(LHV_f\right)$ is calculated using standard molar specific enthalpy of devaluation of reactants and products assuming complete fuel combustion. Thermodynamic properties of water and steam at various pressures and temperatures are determined from International Associations for the properties of water and steam (IAPWS) formulation 1997 [6]. As stated earlier in Chapter 3 and Chapter 4, the fuel flow rate ($\dot{m}_f$) supplied to the boiler is an input to the computer program developed for system simulation. Fuel chemical exergy, energy and exergy lost with the boiler leaving flue gas at the exhaust temperature are calculated. The mass flow rate of steam generated in the boiler $\left(\dot{m}_s\right)$ is calculated from energy balance applied to the boiler control volume.

Table 5.1: Assumed values of parameters

Parameter	Value
Fuel flow rate	20 kg/s
Boiler pressure	150 bar
Reheat pressure	30 bar
Condenser pressure	0.1 bar
ST isentropic efficiency	85%
Pump isentropic efficiency	85%
Compressor isentropic efficiency	85%
CT exit water temperature	25°C
Flue gas temperature at boiler exit	300°C
RS condenser (RSC) exit water temperature	30°C
RS evaporator exit water temperature	10°C
VARS absorber exit water temperature	30°C
Chilled water temperature at AC apparatus inlet	10°C
CT inlet air temperature	28°C
CT inlet air relative humidity	60%
CT exit air temperature	35°C
CT exit air relative humidity	75%
Air flow rate through AC apparatus	4 kg/s
AC apparatus inlet air temperature	28°C
AC apparatus exit air temperature	18°C
AC apparatus inlet air relative humidity	60%
AC apparatus exit air relative humidity	45%
VARS generator temperature	80°C
VARS absorber temperature	35°C
VARS condenser temperature	35°C
VARS evaporator temperature	10°C

The power developed by the ST is:

$$\dot{W}_{ST} = \dot{m}_s\left[(h_1 - h_2) + (1-x)(h_3 - h_4) + (1-x-y)(h_4 - h_5)\right] \quad (5.1)$$

Total pump work required for running the BFPs:

$$\dot{W}_{BFP} = \dot{m}_s\left[(1-x-y)(h_7 - h_6) + (1-x)(h_9 - h_8) + x(h_{12} - h_{11})\right] \quad (5.2)$$

The pumping power required for running the two CT side pumps, $\dot{W}_{CTP}$ is calculated considering pipe dimensions, pipe roughness, static lift, water density, water velocity in pipe, frictional and other minor losses as described in Chapter 3. However, the magnitude of $\dot{W}_{CTP}$ in the VCR based CPC is less due to absence of the pipe network

connecting the CT outlet, VARS absorber and the mixing chamber, MC3 configured in the previous VARS based CS configuration (Fig. 3.1) described in Chapter 3. The net power, $\dot{W}_{net}$ developed by the topping VPC is $\dot{W}_{ST}$ minus the total pumping power i.e. the sum of $\dot{W}_{BFP}$, $\dot{W}_{CTP}$ and RS compressor work ($\dot{W}_{COMP}$). The energy efficiency of the power cycle is the ratio of net power developed to the fuel input energy.

$$\eta_I = \frac{\dot{W}_{net}}{\dot{m}_f \times LHV_f} \text{ where, } \dot{W}_{net} = \dot{W}_{ST} - \left(\dot{W}_{BFP} + \dot{W}_{CTP} + \dot{W}_{COMP}\right) \tag{5.3}$$

Similarly the exergy efficiency is the ratio between net plant power and total exergy supplied to the boiler (sum of fuel's chemical exergy and thermo mechanical exergy of air).

$$\eta_{II} = \frac{\dot{W}_{net}}{\dot{E}x_{ch,\,f} + \dot{E}x_{tm,a}} \tag{5.4}$$

The exergy destruction (irreversibility) in various components of the topping RRVPC is calculated as follows:

Total exergy of boiler leaving flue gas is the sum of chemical and thermomechanical exergy as explained in Chapter 4.

$$\dot{I}_{fg} = \dot{E}x_{ch,\,fg} + \dot{E}x_{tm,\,fg} \tag{5.5}$$

Boiler irreversibility:

$$\dot{I}_{boiler} = \dot{E}x_{ch,\,f} + \dot{E}x_{tm,a} - \dot{E}x_{fg} - \dot{m}_s\left[\left(h_1 - h_{13}\right) + \left(1-x\right)\left(h_3 - h_2\right) - T_0\left(s_1 - s_{13}\right) + \left(1-x\right)\left(s_3 - s_2\right)\right] \tag{5.6}$$

Turbine irreversibility:

$$\dot{I}_{ST} = \dot{m}_s T_0\left[\left(s_2 - s_1\right) + \left(1-x\right)\left(s_4 - s_3\right) + \left(1-x-y\right)\left(s_5 - s_4\right)\right] \tag{5.7}$$

Power cycle condenser (PCC) irreversibility:

$$\dot{I}_{PCC} = T_0\left[\dot{m}_{w,PCC} C_{p,w} \log\left(\frac{T_{wo}}{T_{wi}}\right) + \dot{m}_s\left(1-x-y\right)\left(s_6 - s_5\right)\right] \tag{5.8}$$

Irreversibility in BFP1:

$$\dot{I}_{BFP1} = \dot{m}_s T_0 (1 - x - y)(s_7 - s_6) \quad (5.9)$$

Irreversibility in BFP2:

$$\dot{I}_{BFP2} = \dot{m}_s T_o (1 - x)(s_9 - s_8) \quad (5.10)$$

Irreversibility in BFP3:

$$\dot{I}_{BFP3} = \dot{m}_s T_o x (s_{12} - s_{11}) \quad (5.11)$$

Total BFP irreversibility:

$$\dot{I}_{BFP} = \dot{I}_{BFP1} + \dot{I}_{BFP2} + \dot{I}_{BFP3} \quad (5.12)$$

Irreversibility in OWH:

$$\dot{I}_{OWH} = \dot{m}_S T_O [(1 - x)s_8 - y s_4 - (1 - x - y)s_7] \quad (5.13)$$

Irreversibility in CWH:

$$\dot{I}_{CWH} = \dot{m}_S T_O [x(s_{11} - s_2) + (1 - x)(s_{10} - s_9)] \quad (5.14)$$

Irreversibility in MC1:

$$\dot{I}_{MC1} = \dot{m}_s T_o [(1 - x)(s_{13} - s_{10}) + x(s_{13} - s_{12})] \quad (5.15)$$

In the above equations, x and y represent the fractions of steam extracted per kg of steam for the CWH and OWH respectively. The irreversibility in the CT, CTPs and mixing chamber 2 (MC2) is calculated following the same procedure described in chapter 4.

5.6.2 Calculations: bottoming VCRS

A single stage VCRS is coupled as a bottoming cycle with the topping RRVPC. In the VCRS, the refrigerant R−134a (1, 1, 1, 2−tetrafluoroethane) is used as working fluid. The CT in the combined system not only assists in supplying cold water to the power cycle condenser (PCC), but also helps in supplying cold water through the VCRS condenser and the evaporator (also the AC apparatus). The water circulated through the

evaporator provides the latent heat of vaporization required for evaporation of R134a in the VCRS evaporator. Since the temperatures of water at evaporator inlet and outlet are specified, the mass flow rate of water can be calculated from heat balance in the evaporator. The chilled water thus produced in the evaporator flows through the AC apparatus to cool and dehumidify the hot and humid air. Mass flow rate of moist air, its DBT and RH at inlet and exit of the AC apparatus are specified. Therefore, from known values of chilled water flow rate and its inlet temperature, the temperature of water at the AC apparatus outlet can be determined from energy balance in the AC apparatus. Similarly the water flow rates through the PCC and VCRS condenser are also determined from energy balance applied to these devices. Inlet and outlet temperatures of water to these devices are known (refer Table 5.1). The water from the PCC, VCRS condenser and the AC apparatus; all go to the mixing chamber (MC2). The temperature of the mixed water stream is calculated from the SFEE applied to MC2.

The temperature and pressure dependent thermodynamic properties of R−134a are calculated using equations taken from the Ref. [7]. Density of R−134a at a given temperature is calculated using the Newton−Raphson iterative method with an initial guess value of density calculated from the ideal gas equation. The following values of gas constant (R), critical temperature (T_c) and critical density (ρ_c) are taken.

$$R = 81.488856 \text{ J/kgK};\ T_c = 374.18 \text{ K};\ \rho_c = 508 \text{ kg/m}^3$$

VCRS CL is specified as a model input parameter from which the mass flow rate of refrigerant is calculated as follows.

$$\dot{m}_r = \frac{\dot{Q}_E}{h_4' - h_3'} \tag{5.16}$$

Compressor work is calculated using the following relation.

$$\dot{W}_{COMP} = \dot{m}_r (h_1' - h_4'), \tag{5.17}$$

The COP of the VCRS is:

$$COP = \frac{\dot{Q}_E}{\dot{W}_{COMP}} \tag{5.18}$$

The maximum (Carnot) COP and exergy efficiency of the VCRS are defined as follows:

$$COP_{carnot} = \frac{T_E}{T_C - T_E} \tag{5.19}$$

$$\text{VCRS exergetic efficiency} = \frac{\dot{E}x_{w,Eo} - \dot{E}x_{w,Ei}}{\dot{W}_{COMP}} \tag{5.20}$$

The EUF of the CPC system is:

$$EUF = \frac{\dot{W}_{net} + \dot{Q}_E}{\dot{m}_f \times LHV_f} \tag{5.21}$$

Exergetic efficiency of the CS is defined by the following equation.

$$\eta_{II,CS} = \frac{\dot{W}_{net} + \dot{E}x_{w,Eo} - Ex_{w,Ei}}{\dot{E}x_{ch,f} + \dot{E}x_{tm,a} + \dot{W}_{COMP}} \tag{5.22}$$

Same formulae as specified in Chapter 4 are used for calculation of exergy destruction/irreversibility in the VCRS condenser, expansion valve, evaporator and the AC apparatus. The irreversibility in the compressor is calculated using the following equation.

$$\dot{I}_{COMP} = \dot{m}_r T_0 \left(s_1' - s_4'\right) \tag{5.23}$$

The total irreversibility of the combined power and VCRS based cooling system is the sum of irreversibility in all components of the combined system.

5.7 Performance comparison of the CS with VARS and VCRS as bottoming cycles

A detailed energy and exergy based parametric analysis of the combined RRVPC and the single effect H_2O−LiBr VARS was presented in Chapter 3 and Chapter 4. All these parametric variations would be unnecessary for the CS with the VCRS as bottoming cycle. Since, it is the bottoming cooling cycle that would be different in the two combined systems, hence, the performance comparison of the two combined systems is provided in terms of evaporator cooling load (CL) variation of the VARS and VCRS.

5.7.1 Performance comparison as function of evaporator CL

Performance comparison of the two combined systems as function of evaporator CL is shown in Table 5.2. The net power output of the topping RRVPC of both the combined systems reduces with increase in CL. As can be seen from the results in Table 5.2, the total BFP pumping power of the two combined systems does not change with cooling load and BFP pumping power requirement is slightly less in the VCR based CS. On the other hand, the total CTP pumping power increases with cooling load in both the systems and the CTP pumping power requirement is less in the VCR based CS at a particular cooling load. SP power of the VARS and compressor power $\left(\dot{W}_{COMP}\right)$of the VCRS also increases with increase in cooling load. But overall the total power requirement is less for the VCR based CS at a particular cooling load. Again, the ST power $\left(\dot{W}_{ST}\right)$is also more for the VCR based CS and it does not change much with CL in case of the VCR based CS. In the VCR based CS, $\dot{W}_{ST}$ value remains fixed with cooling load and $\dot{W}_{ST}$ is 190.437 MW at BP 150 bar, FFR 20 kgs^{-1}, T_E =10°C and T_C =35°C. Net power of the topping RRVPC of the VCR based CS reduces with cooling load only due to increase in CTP pumping power and $\dot{W}_{COMP}$ at higher cooling loads. However in the VAR based system, the ST power slightly decreases with increase in CL because more steam is required to be extracted from the ST due to increase in generator heat load at higher evaporator CL and this causes a reduction in ST power.

The energy and exergy efficiency of the topping RRVPC reduces marginally with evaporator CL in both the combined systems. The heat loss in the PCC shows a decreasing trend with increase in evaporator CL in the VAR based CS due to reduction in the steam flow rate through the condenser as certain amount of steam is extracted from the ST to supply the heat required for vapor generation in the VARS generator. The heat loss in the PCC however does not change with evaporator CL in the VCR based CS but comparatively more heat loss occurs. The COPs (actual and Carnot) and also the exergetic efficiency of the two refrigeration systems is not a function of the evaporator CL, hence they remain constant however performance wise, VCRS outperforms the VARS. EUF and exergy efficiency of the two systems increase marginally with evaporator CL in spite of reduction in net power value, but again their magnitudes are higher for the CS with VCRS at a given CL.

Table 5.3 shows irreversible losses occurring in various components of the CS integrated with VCRS and VARS. Irreversibility results show that irreversible losses in the ST, PCC, OWH, CT and MC1 of the VAR based CS decreases with evaporator CL while these losses in MC3 and the CTPs are more at higher CL. Irreversibility in the boiler, CWH, BFP and the exhaust irreversibility are not affected by CL variation. However in the VCR based CS, irreversible losses in most of the power cycle components remain invariant with CL except in the CT, CTPs and MC2. Like in the VAR based CS, in the VCR based system also; CT irreversibility decreases while CTP and MC2 irreversibility increases with increase in CL. It may be reiterated that MC2 in Fig. 5.1 in this chapter is identical with MC3 in Fig. 3.1 of Chapter 3. Compared to the VAR based CS, the irreversible losses in the ST, OWH, CT and CTPs of the VCR based CS are less while the boiler, PCC, BFP irreversibility are more in the VCR based CS.

Irreversibility in the CWH and exhaust gas irreversibility of the two systems are exactly same at various CLs. But as stated earlier, the main difference arises due to irreversibility in the mixing chambers of the two systems; the losses are significantly less in the CS integrated with VCRS. This is why the total irreversible loss in the power cycle components of the VCR based CS is less. Again considering the irreversible losses in the refrigeration system alone, it is seen that these losses increase with CL in both the VARS and VCRS, but the total irreversible losses of the RS components alone is less in the VCRS. The irreversibility in the generator, SHE, SP and absorber of the VARS increases with CL and the sum of irreversibility in all these components at a given CL is higher than the compressor irreversibility $\left(\dot{I}_{COMP}\right)$. The total irreversible losses of the two systems as a function of CL is shown in Fig. 5.3 and it is seen that the total irreversible loss is less for the VCR based CS and also the difference between total irreversibility of the two systems increases with increase in CL.

Table 5.2: Comparison of performance of the CS with VARS and VCRS at various cooling loads

Parameter	Evaporator cooling load									
	7000 kW		8750 kW		10500 kW		12250 kW		14000 kW	
	With VARS	With VCR	With VARS	With VCR	With VARS	With VCR	With VARS	With VCR	With VARS	With VCR
Net power (MW)	178.614	182.348	178.11	181.941	177.577	181.522	177.014	181.091	176.418	180.647
Steam generation rate (kg/s)	170.024	169.609	170.024	169.609	170.024	169.609	170.024	169.609	170.024	169.609
BFP pumping power (MW)	3.145	3.138	3.145	3.138	3.145	3.138	3.145	3.138	3.145	3.138
CT side pumping power (MW)	4.555	4.120	4.876	4.320	5.227	4.531	5.609	4.755	6.023	4.991
Solution pump power (W)	59.1	–	73.9	–	88.7	–	103.5	–	118.2	–
$\dot{W}_{COMP}$ (W)		830.367		1037.959		1245.551		1453.142		1660.734
Energy efficiency of VPC (%)	35.999	34.748	35.898	34.661	35.791	34.573	35.677	34.481	35.557	34.387
Exergy efficiency of VPC (%)	33.945	32.786	33.849	32.705	33.748	32.621	33.641	32.535	33.528	32.446
COP	0.813	8.43	0.813	8.43	0.813	8.43	0.813	8.43	0.813	8.43
Exergetic efficiency of RS (%)	11.817	21.945	11.817	21.945	11.817	21.945	11.817	21.945	11.817	21.945
EUF of the CS	0.374	0.382	0.377	0.384	0.379	0.387	0.381	0.390	0.384	0.392
Exergy efficiency of CS (%)	33.880	32.767	33.769	32.68	33.652	32.592	33.53	32.501	33.401	32.408

Table 5.3: Comparison of component irreversibility of the CS with VARS and VCRS at various cooling loads

Irreversibility	Evaporator cooling load									
	7000 kW		8750 kW		10500 kW		12250 kW		14000 kW	
	With VARS	With VCR	With VARS	With VCR	With VARS	With VCR	With VARS	With VCR	With VARS	With VCR
$\dot{I}_{boiler}$ (kW)	117151.134	115680.002	117151.134	115680.002	117151.134	115680.002	117151.134	115680.002	117151.134	115680.002
$\dot{I}_{ST}$ (kW)	22383.206	19408.981	22318.381	19408.981	22253.556	19408.981	22188.730	19408.981	22123.905	19408.981
$\dot{I}_{PCC}$ (kW)	10175.496	10416.642	10091.686	10416.642	10007.876	10416.642	9924.066	10416.642	9840.255	10416.642
$\dot{I}_{BFP}$ (kW)	219.277	248.451	219.290	248.451	219.301	248.451	219.313	248.451	219.325	248.451
$\dot{I}_{OWH}$ (kW)	4478.066	4085.312	4456.763	4085.312	4435.459	4085.312	4414.154	4085.312	4392.850	4085.312
$\dot{I}_{CWH}$ (kW)	3611.462	3602.665	3611.462	3602.665	3611.462	3602.665	3611.462	3602.665	3611.462	3602.665
$\dot{I}_{MC1}$ (kW)	7778.544	0.000	7766.777	0.000	7754.907	0.000	7742.936	0.000	7730.863	0.000
$\dot{I}_{MC2}$ (kW)	0.000	843.169	0.000	1037.571	0.000	1225.512	0.000	1407.348	0.000	1583.510
$\dot{I}_{MC3}$ (kW)	1000.599	–	1213.883	–	1414.475	–	1603.638	–	1782.470	–
$\dot{I}_{fg}$ (kW)	177232.742	177232.742	177232.742	177232.742	177232.742	177232.742	177232.742	177232.742	177232.742	177232.742
$\dot{I}_{CT}$ (kW)	16164.111	16296.672	16000.494	16182.954	15850.281	16076.123	15712.230	15975.708	15585.261	15881.282
$\dot{I}_{CTP}$ (kW)	17120.790	12112.686	18145.677	12551.956	19335.934	13089.505	20660.367	13698.943	22103.872	14366.679
$\dot{I}_{RSC}$ (kW)	194.641	191.230	243.302	239.038	291.962	286.845	340.622	334.653	389.282	382.460
$\dot{I}_{E}$ (kW)	188.612	188.604	235.766	235.755	282.919	282.906	330.072	330.057	377.225	377.208
$\dot{I}_{ExV}$ (kW)	13.561	83.674	16.952	104.593	20.343	125.511	23.733	146.429	27.123	167.348
$\dot{I}_{COMP}$ (kW)	–	119.702	–	149.627	–	179.552	–	209.478	–	239.403
$\dot{I}_{SHE}$ (kW)	35.342	–	41.177	–	53.013	–	61.848	–	70.684	–
$\dot{I}_{SP}$ (kW)	0.054	–	0.068	–	0.081	–	0.095	–	0.108	–
$\dot{I}_{G}$ (kW)	2252.551	–	2815.688	–	3378.826	–	3941.963	–	4505.101	–
$\dot{I}_{A}$ (kW)	403.169	–	503.962	–	604.754	–	705.546	–	806.339	–
$\dot{I}_{AC}$ (kW)	1.939	1.939	1.958	1.958	1.971	1.971	1.982	1.982	1.992	1.992

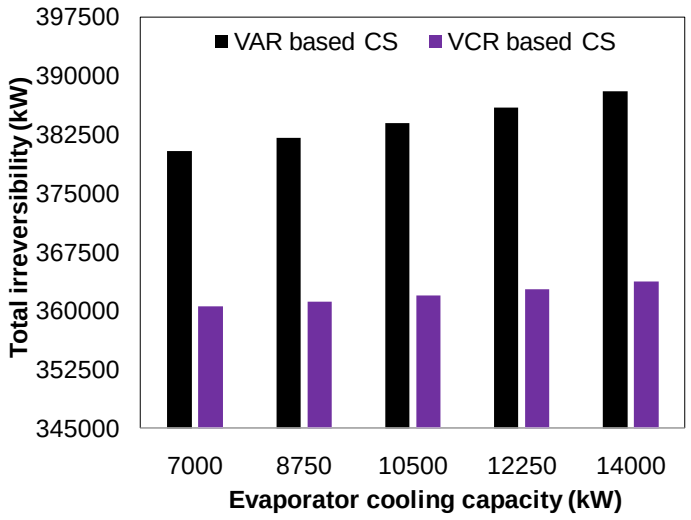

Fig. 5.3: Total system irreversibility variation of the VAR and VCR based CS with evaporator CL

5.7.2 Performance comparison at fixed CL of 14000 kW at T_E =5°C

To understand better the difference in performance of the CS separately with the VCRS and the VARS as bottoming cycle, particularly at a given evaporator CL, the simulation was also performed at another evaporator temperature i.e. at T_E =5°C while keeping the CL fixed at 14000 kW. Table 5.4 shows the performance comparison of the CS with VARS and VCRS at the given operating conditions.

It was seen that compared to the VAR based CS, the net power output of the VCR based CS is more although the steam generation rate in the boiler is slightly less for the CS integrated with VCRS. The BFP pumping power of the VCR based CS is only marginally less compared to that of the VAR based CS although there is one less number of BFP in the VCR based CS. However, the pumping power required for running the CTPs is significantly less in the VCR based CS compared to the VAR based CS. This is mainly due to water mass flow rate which is less in the VCR based CS because no water is required to be circulated through the absorber as required in the VAR based CS.

The frictional loss in the VCR based CS is also less due to absence of the pipe network that was additionally required in the VAR based CS to supply water from the CT exit to the absorber and the MC3 (see Fig.3.1 in Chapter 3). Obviously the compressor

power requirement of the VCRS is more than the SP power requirement in the VARS, but overall the total pumping power requirement is less in the VCR based CS. Also the ST power developed in the VCR based CS is more because no steam from ST is extracted here as it is required in the VAR based CS for supplying the heat for vapor generation in the generator. Therefore, the net power output is more from the topping power cycle of the VCR based CS. Slight change in the steam generation rate in the two CSs is due to difference in values of enthalpy at state points 13 and 17 in Fig. 5.1 and Fig. 3.1 respectively. Since the net power is more in the VCR based CS for the same fuel input energy and exergy supplied to the boiler, hence the energy and exergy efficiencies are also more in case of the VCR based CS. It is seen that with the VCRS as bottoming cycle, the energy losses in the PCC condenser is more. This is mainly due to condensation of relatively more amount of steam in the condenser because no steam is extracted from the ST.

In the bottoming cooling system, it is observed that the COPs (both actual and Carnot) are significantly higher in case of the VCRS. Higher COP in case of VCRS is obvious due to lower magnitude of $\dot{W}_{COMP}$ compared to $\dot{Q}_G$. In the VCRS, more refrigerant is required to achieve the same amount of cooling. Again it was observed that the VCRS exergy efficiency is also more compared to VARS. EUF of the VCR based CS is slightly more due to higher net power output from the power cycle. The exergy efficiency of the VCR based CS is more compared to the VAR based CS.

Table 5.5 shows irreversible losses occurring in various components of the CS integrated with the VARS and the VCRS. In the VCR based CS, the irreversible losses in the boiler, condenser, CT, BFPs of the power cycle components and expansion valve of the RS are more compared to losses in the respective components of the VAR based CS. However, these losses in the ST, OWH, CTPs and refrigeration system condenser (RSC) are less, particularly in the CTPs. Irreversibility of the CWH, exhaust flue gas and the AC apparatus in the two systems are exactly the same. Evaporator irreversibility is also more or less the same in both the systems. Irreversibility of the VCRS compressor is also significantly less (300.775 kW) compared to that of the generator−solution heat exchanger (SHE)−SP−absorber assembly of the VAR based CS (total 5464.072 kW). The difference in total irreversibility also arises due to the irreversible losses of the mixing chambers. There

are two and three mixing chambers respectively in the VCR based CS (Fig. 5.1) and VAR based CS (Fig. 3.1 shown in Chapter 3). Therefore irreversible losses occurring in the mixing chambers of the VCR based CS (Fig. 5.1) are less compared to irreversibility of mixing chambers in the VAR based CS (Fig. 3.1shown in Chapter 3). This ultimately results in lower total system irreversibility in the VCR based CS.

Table 5.4: Performance comparison of the CS with VARS and VCRS as bottoming cycles (T_E =5°Cand $\dot{Q}_E$ =14000 kW)

Parameters	With VARS	With VCRS
Net power (MW)	176.272	180.196
Steam generation rate (kg/s)	170.024	169.609
BFP pumping power (MW)	3.145	3.138
CT side pumping power (MW)	6.091	5.028
Solution pump power (W)	202.5	–
$\dot{W}_{COMP}$ (W)	–	2075.188
Energy efficiency of VPC (%)	35.528	36.319
Exergy efficiency of VPC (%)	33.500	34.269
VPC condenser loss (kW)	238832.214	253749.675
COP(Actual)	0.771	6.746
COP (Carnot)	1.181	9.270
$\dot{m}_r$ (kg/s)	5.924	91.801
$\dot{m}_{LiBr}$ (kg/s)	38.018	–
$\dot{Q}_{RSC}$ (kW)	14829.0	16075.0
Exergetic efficiency of RS (%)	11.215	17.562
EUF of the CS	0.383	0.391
Exergy efficiency of CS (%)	33.363	34.203

Table 5.5: Comparison of component irreversibility of the CS with VARS and VCRS as bottoming cycles (T_E =5°C and $\dot{Q}_E$ =14000 kW)

Irreversibility (kW)	With VARS	With VCRS
$\dot{I}_{boiler}$	117151.134	115680.003
$\dot{I}_{ST}$ (kW)	22096.070	19408.981
$\dot{I}_{PCC}$ (kW)	9804.268	10416.642
$\dot{I}_{BFP}$ (kW)	219.330	248.451
$\dot{I}_{OWH}$ (kW)	4383.703	4085.312
$\dot{I}_{CWH}$ (kW)	3611.462	3602.665
$\dot{I}_{MC1}$ (kW)	7725.648	0.000
$\dot{I}_{MC2}$ (kW)	0.000	1590.256
$\dot{I}_{MC3}$ (kW)	1791.842	–
$\dot{I}_{fg}$ (kW)	177232.742	177232.742
$\dot{I}_{CT}$ (kW)	15567.446	15897.215
$\dot{I}_{CTP}$ (kW)	22353.832	14514.096
$\dot{I}_{RSC}$ (kW)	390.791	395.746
$\dot{I}_{E}$ (kW)	642.219	642.203
$\dot{I}_{ExV}$ (kW)	40.145	242.163
$\dot{I}_{COMP}$ (kW)	–	300.775
$\dot{I}_{SHE}$ (kW)	121.486	
$\dot{I}_{SP}$ (kW)	0.186	
$\dot{I}_{G}$ (kW)	4598.718	
$\dot{I}_{A}$ (kW)	743.682	
$\dot{I}_{AC}$ (kW)	1.992	1.992

5.8 Summary

The observations from this comparative analysis can be summarized as follows.

From CL variation it was found that the net power of the toping RRVPC reduces with increase in CL in both the systems. Irreversible losses in the ST, PCC, OWH, CT and MC1 of the VAR based CS decreases with CL while in the VCR based CS, irreversible losses in most of the power cycle components remain invariant with CL except in the CT,

CTPs and MC2. It was also seen that the irreversible losses are less in power cycle components of the VCR based CS. The losses in the RS components increase with CL in both the VARS and VCRS, but the total irreversible losses of the RS components alone are less in the VCRS. It was found that the compressor irreversibility is much lower than the total irreversible losses in the generator−solution heat exchanger (SHE)−SP−absorber assembly of the VARS. Consequently the total system irreversibility of the VCR based CS becomes less than that of the VAR based system at all CLs. Among the VCRS components the condenser produces the highest irreversibility followed by the evaporator, compressor and the expansion valve.

Compared to the VAR based CS, the BFP pumping power is slightly less while the CTP pumping power is significantly less in the VCR based CS. This reduction in CTP pumping power in the VCR based CS is caused by the change in water mass flow rate which is significantly less in the VCR based system due to absence of the absorber which in the VARS requires cold water circulation to absorb the heat released during exothermic reaction between water vapor and LiBr salt. The CTP pumping power is also less in the VCR based CS due to lower frictional head loss caused by the absence of the pipe network from the CT outlet connecting the absorber and the mixing chamber (MC3) of the VAR based CS. Although the compressor power of the VCRS is more than the solution pump (SP) power of the VARS, but reduction in the BFP and CTP pumping power, particularly the CTP pumping power caused a significant reduction in the total negative power requirement in the VCR based CS. Power developed in the ST is also more in the VCR based CS due to the fact that steam is not extracted here as it is done in the VAR based system to provide the generator heat load. Hence the net power output from the topping RRVPC is more in the VCR based system compared to that of the VAR based CS.

Accordingly the power cycle energy and exergy efficiencies of the VCR based CS are higher than those of the VAR based system. Moreover, a given cooling effect is produced with much higher COP and exergetic efficiency with VCRS and most importantly this is done with significant gain in the net power output from the topping RRVPC.

The total irreversibility of the power cycle components is less in the VCR based CS due to irreversibility difference caused by one extra mixing chamber (MC1 in Fig. 3.1) in the VAR based system.

Irreversible losses in the components of the cooling systems are also less in case of the VCRS because of compressor irreversibility which is lower than the total losses in the generator−solution heat exchanger (SHE)−SP−absorber assembly of the VARS. Consequently the total system irreversibility of the VCR based CS becomes less than that of the VAR based system at all operating conditions. Among the VCRS components the condenser produces the highest irreversibility followed by the evaporator, compressor and the expansion valve.

Finally it can be summarized that among the two combined power and cooling systems, the system with VCRS may be preferred if higher net power output and minimum total system irreversibility are the sole criteria. Definitely the cost of the VCR based CS will be less than that of the VAR based system. The VAR based combined configuration may also be useful in case when excess steam is produced and lost unused in the plant. If cooling is at all to be produced by using VARS without losing much power from the power cycle, the exhaust heat of the boiler leaving flue gas could be a an option as a source of heat for operating the VARS.

List of References

[1] Llopis, R., Sánchez, D., Sanz−Kock, C. S., Cabello, R.,and Torrella, E. Energy and environmental comparison of two−stage solutions for commercial refrigeration at low temperature: Fluids and systems. *Applied Energy*, 138:133–142, 2015.

[2] Trygg, L. and Amiri,S. European perspective on absorption cooling in a combined heat and power system – A case study of energy utility and industries in Sweden. *Applied* Energy, 84(12): 1319–1337, 2007.

[3] Elsafty, A., Al−Daini, A. J. Economical comparison between a solar powered vapour absorption air−conditioning system and a vapour compression system in the Middle East. *Renewable Energy*, 25: 569–583, 2002.

[4] Riffat,S. B. and Qiu,G. Comparative investigation of thermoelectric air−conditioners versus vapour compression and absorption air−conditioners. *Applied Thermal Engineering*, 24: 1979–1993, 2004.

[5] Muangnoi, T., Asvapoositkul. W.,andWongwises, S. An exergy analysis on the performance of a counter flow wet cooling tower. *Applied Thermal Engineering*, 27:910–917, 2007.

[6] Wagner, W., Cooper, J.R., Dittmann, A., Kijima, J., Kretzschmar, H.J., and Kruse, A. The IAPWS Industrial Formulation 1997 for the thermodynamic properties of water and steam. *Journal of Engineering for Gas Turbines and Power*, 122:150–182, 2000.

[7] Baehr,H.D.,andTillner−Roth,R. *Thermodynamic properties of environmentally acceptable refrigerants*, Springer−Verlag Berlin Heidelberg, 1st edition. 1995.